RSC Advances

PAPER

Cite this: *RSC Adv.*, 2015, **5**, 18359

High performance composite polymer electrolytes for lithium-ion polymer cells composed of a graphite negative electrode and $LiFePO_4$ positive electrode

Yoon-Sung Lee, Won-Kyung Shin, Jung Soo Kim and Dong-Won Kim*

Received 4th December 2014
Accepted 5th February 2015

DOI: 10.1039/c4ra15767b

www.rsc.org/advances

Core–shell structured SiO_2 particles with different core diameters were synthesized by radical polymerization of 4-styrenesulfonic acid sodium salt with vinyl-functionalized SiO_2 core particles and were used as Li^+ ion-conducting fillers in composite polymer electrolytes. Composite polymer electrolytes prepared with core–shell SiO_2 particles exhibited high ionic conductivity exceeding 10^{-3} S cm^{-1} at room temperature and good mechanical properties, allowing the preparation of a free-standing film with a thickness of 30 μm. Lithium-ion polymer cells composed of graphite negative electrode, composite polymer electrolyte and $LiFePO_4$ positive electrode were assembled, and their cycling performance was evaluated. Cells assembled with a composite polymer electrolyte containing core–shell SiO_2 particles with a core diameter of 250 nm exhibited good cycling performance in terms of discharge capacity, capacity retention and rate capability.

Introduction

Rechargeable lithium-ion polymer batteries employing polymer electrolytes have been actively investigated for application in portable electronic devices, electric vehicles and energy storage systems.[1–5] The use of a polymer electrolyte enables fabrication of safe batteries and permits leakage-proof construction with design flexibility. In addition, lithium-ion polymer batteries can be packaged in plastic pouches, thereby improving the specific energy of the battery. Attempts to obtain solid polymer electrolytes consisting of a matrix polymer and a lithium salt have thus far only yielded electrolytes with limited ionic conductivity at ambient temperature.[6–8] It has been reported that the addition of polar organic solvents into matrix polymers such as polyacrylonitrile (PAN), poly(vinylidene fluoride) (PVdF), poly(vinylidene fluoride-*co*-hexafluoropropylene) (P(VdF-*co*-HFP)), and poly(methyl methacrylate) (PMMA) can significantly increase their ionic conductivity.[9,10] Such gel polymer electrolytes exhibit high ionic conductivities exceeding 10^{-3} S cm^{-1} at room temperature. However, their mechanical properties are often very poor, which is one of the most important deficiencies preventing their practical application in cells. Thus, porous polyolefin separators are currently being used as mechanical supports in commercialized lithium-ion polymer batteries that employ gel polymer electrolytes. To obtain gel polymer electrolytes with improved mechanical properties without a mechanical support, inert ceramic fillers such as SiO_2, Al_2O_3, TiO_2, and $BaTiO_3$ have been incorporated into gel polymer electrolytes.[11–17] Incorporation of nanosized ceramic particles into the gel polymer electrolytes improves their mechanical strength through physical action without directly contributing to the lithium-ion transport process. Surface modification of these ceramic fillers allows them to serve as a source of Li^+ ions.[18,19] In previous studies, we synthesized core–shell structured SiO_2 particles composed of an inorganic SiO_2 core and an organic polymer shell, and used these particles as functional fillers in composite polymer electrolytes.[20–22] In these particles, poly(lithium-4-styrenesulfonte) is covalently bonded to the SiO_2 core. The Li^+ ions in poly(lithium-4-styrenesulfonte) of the core–shell structured SiO_2 particles contribute to Li^+-ion conductivity. We described the effect of the shell thickness of the core–shell structured SiO_2 particles on the electrochemical properties of the composite polymer electrolytes in a previous report.[22] Encouraged by previous studies, the effect of SiO_2 core size on the cycling performance of lithium-ion polymer cells is of great interest, because the electrochemical properties of the composite polymer electrolytes can be affected by core size of nano-engineered silica particles containing lithium ions.

In this study, we synthesized core–shell structured SiO_2 particles with different core size, but the same shell thickness. $SiO_2(Li^+)$ particles were incorporated into a P(VdF-*co*-HFP) copolymer to make a composite polymer membrane, and the membrane was activated by soaking with liquid electrolyte to prepare the composite polymer electrolyte. Composite polymer

Department of Chemical Engineering, Hanyang University, Seongdong-Gu, Seoul 133-791, Republic of Korea. E-mail: dongwonkim@hanyang.ac.kr; Fax: +82 2 2220 4337; Tel: +82 2 2220 2337

electrolytes were applied to lithium-ion polymer cells composed of a graphite negative electrode and a $LiFePO_4$ positive electrode. The cycling performances of the cells were evaluated and compared to those of cells assembled with liquid electrolyte. We performed a detailed investigation of the effect of core size on cycling performance in order to provide the optimized composite polymer electrolytes for high performance lithium-ion polymer cells.

Experimental

Synthesis of core–shell structured $SiO_2(Li^+)$ nanoparticles

The three-step synthetic scheme used to prepare core–shell structured SiO_2 particles with different core sizes is illustrated in Fig. 1. An appropriate amount of vinyltrimethoxysilane (VTMS, Evonik) was added to double distilled water while stirring until the VTMS droplets completely disappeared. A catalytic amount of ammonium hydroxide solution (28 wt% NH_4OH, Junsei) was added to the solution, and the sol–gel reaction (hydrolysis and condensation) was allowed to proceed for 12 h at ambient temperature. After completion of the reaction, the resulting precipitate (silica core with vinyl groups) was centrifuged and washed several times with ethanol. Vinyl-functionalized SiO_2 core particles with diameters ranging from 250 to 810 nm were obtained. Core–shell structured $SiO_2(Na^+)$ particles were synthesized by radical copolymerization of silica core particles and 4-styrenesulfonic acid sodium salt (Sigma-Aldrich) with azobisisobutyronitrile in *n*-methyl pyrrolidone (NMP) at 60 °C for 72 h. After polymerization, the resulting solution was precipitated into a large excess of diethyl ether with vigorous stirring. The precipitate was filtered and washed with methanol several times. Na^+ ions in poly(sodium-4-styrenesulfonte) of the shell were replaced with Li^+ ions by ionic exchange with $LiOH \cdot H_2O$. The resulting $SiO_2(Li^+)$ particles were washed with ethanol to remove any impurities and core–shell structured $SiO_2(Li^+)$ particles were obtained as white powders after vacuum drying at 110 °C for 12 h.

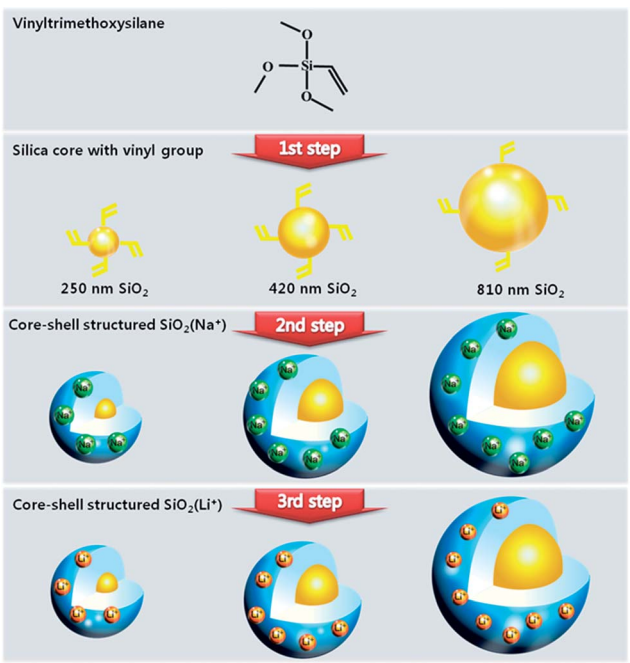

Fig. 1 Schematic reaction scheme for synthesis of core–shell structured $SiO_2(Li^+)$ particles with different core diameters.

Preparation of composite polymer electrolytes

Composite polymer film consisting of P(VdF-*co*-HFP) (Kynar 2801, M_w = 380 000) and core–shell structured $SiO_2(Li^+)$ particles was prepared by mixing P(VdF-*co*-HFP), $SiO_2(Li^+)$ particles and dibutyl phthalate (DBP) in acetone by ball milling and subsequent casting using a doctor blade. After solvent evaporation for 30 min, the film was immersed in methanol to form pores by removal of DBP. The resulting porous membrane was vacuum-dried at 70 °C for 12 h. The content of core–shell $SiO_2(Li^+)$ particles in the composite polymer membrane was fixed at 20 wt% based on the weight of polymer membrane containing P(VdF-*co*-HFP) and $SiO_2(Li^+)$ particles, because in our previous study, we found that 20 wt% was the optimum content for achieving high conductivity.[20] The thickness of the composite polymer membrane was about 30 μm. Composite polymer electrolytes were finally obtained by soaking the membranes in 1.15 M $LiPF_6$–ethylene carbonate (EC)/diethyl carbonate (DEC) (3 : 7 by volume, battery grade, Soulbrain Co.). Uptake of the electrolyte solution in the composite polymer electrolyte was determined by the following equation: uptake (%) = $[(W_c - W_m)/W_m] \times 100$, where W_c and W_m are the weights of the composite polymer electrolyte and dry composite membrane, respectively.

Electrode preparation and cell assembly

We used $LiFePO_4$ as an active material in the positive electrode due to its good cycleability, low cost, low toxicity and high thermal stability.[23–26] The $LiFePO_4$ electrode was prepared by coating a NMP-based slurry containing $LiFePO_4$ powder (Top Battery Co.), PVdF (KF-1300, Kureha) and super-P carbon (MMM Co.) (92 : 4 : 4 by weight) onto Al foil. Its active mass loading corresponded to a capacity of about 2.0 mA h cm^{-2}. The carbon electrode was similarly prepared by coating a NMP-based slurry of mesocarbon microbeads (MCMB, Osaka Gas), PVdF, and super-P carbon (88 : 8 : 4 by weight) onto Cu foil. Lithium-ion polymer cell was assembled by sandwiching the composite polymer electrolyte between the graphite negative electrode and the $LiFePO_4$ positive electrode. The cell was enclosed in a metalized plastic pouch and was vacuum-sealed in a glove box filled with argon gas. For comparison, a liquid electrolyte-based lithium-ion cell with a polypropylene separator (Celgard 2400) and the same liquid electrolyte (1.15 M $LiPF_6$–EC/DEC) instead of a composite polymer electrolyte was also assembled.

Measurements

Morphologies of the silica core particles and composite polymer membranes were examined using a field emission scanning electron microscope (FE-SEM, JEOL JSM-6330F). Fourier transform infrared (FT-IR) spectra of vinyl-functionalized SiO_2 core

particles and core–shell structured SiO_2 particles were recorded on a Magna IR 760 spectrometer with KBr powder-pressed pellets. Core–shell structured SiO_2 particles were characterized by a field emission transmission electron microscope (FE-TEM, FEI JEM 2100F) equipped with energy dispersive X-ray spectroscopy (EDS). The mechanical properties of the composite polymer membranes were measured using a universal test machine (Instron 5966) in accordance with the ASTM D882 method. AC impedance measurements were performed to measure the ionic conductivities of composite polymer electrolytes using a Zahner Electrik IM6 impedance analyzer over the frequency range of 10 Hz to 100 kHz with an amplitude of 10 mV. The lithium transference number was measured by a combination of AC impedance and DC polarization methods.[27] Charge and discharge cycling tests of the lithium-ion polymer cells were conducted at a current of 0.5C rate over the voltage range of 2.0–3.7 V using battery testing equipment (WBCS 3000, Wonatech) at room temperature. The rate capability of the cells was investigated at different current rates from 0.1 to 2.0C.

Results and discussion

FE-SEM images of vinyl-functionalized SiO_2 particles obtained by the sol–gel reaction of VTMS in aqueous solution are shown in Fig. 2. All silica particles had uniform spherical shapes with average diameters of about 250, 420 and 810 nm, respectively. The particle size of the silica cores was controlled by changing the concentration of VTMS in the first synthetic step depicted in Fig. 1. The chemical structure of vinyl-functionalized SiO_2 particles was confirmed by FT-IR spectroscopy. As can be seen in Fig. 3(a)–(c), the SiO_2 particles showed a characteristic broad band associated with asymmetric stretching vibrations of the siloxane (Si–O–Si) around 1100 cm^{-1}. The presence of C=C double bonds introduced by the covalently bonded VTMS molecules in the SiO_2 particles was confirmed by two peaks at 1410 and 1603 cm^{-1}, which are characteristic of C=C double bonds,[28–30] indicating that the silica particles contained vinyl groups. These vinyl groups permitted further reaction of silica core particles with 4-styrenesulfonic acid sodium salt during the second step to produce core–shell structured silica particles. The peak intensity of the C=C double bond slightly decreased with increasing SiO_2 core particle size, which implies that reactive sites on the SiO_2 core particle for free radical copolymerization with 4-styrenesulfonic acid sodium were more abundant in SiO_2 core particles with smaller diameters than those with larger diameters. In the core–shell structured SiO_2 particles (Fig. 3(d)), the peak intensities of C=C double bond were decreased as compared to those of SiO_2 core particles (Fig. 3(a)), indicating the vinyl groups on the cored SiO_2 particles were reacted with 4-styrenesulfonic acid sodium salt by radical polymerization to produce core–shell structured SiO_2 particles. New peaks were observed at 1041 and 1186 cm^{-1}, which can be assigned to the symmetric and asymmetric vibration of SO_3^- group, respectively.[31] In-plane skeleton vibration peak of benzene ring was appeared at 1130 cm^{-1}, while in-plane bending vibration peak of benzene ring was observed at 1010 cm^{-1}.[31,32] From the above results, it was confirmed that poly(sodium-4-styrenesulfonate) was covalently bonded to SiO_2 core particle.

TEM images of core–shell structured SiO_2 particles containing poly(sodium-4-styrenesulfonte) in the shell are shown in Fig. 4. All particles had extremely uniform core–shell morphologies with a shell layer of poly(sodium-4-styrenesulfonte) surrounding a SiO_2 core particle. The thickness of the shell layer in the core–shell structured SiO_2 particles was about 250 nm. SiO_2 core diameters were consistent those of the SiO_2 core particles shown in Fig. 2. These results confirmed that the SiO_2 particles were well encapsulated by a poly(sodium-4-styrenesulfonte) layer with a uniform thickness and that spherical core–shell structured SiO_2 particles were successfully synthesized. Sodium ions in

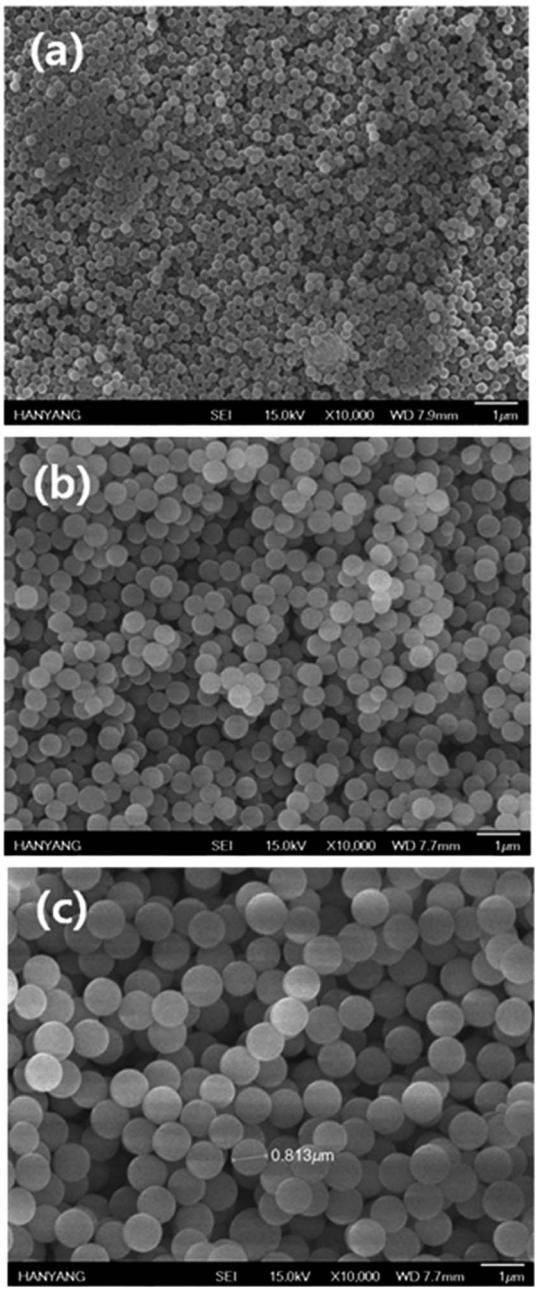

Fig. 2 SEM images of SiO_2 core particles with different diameters. Average diameters are (a) 250 nm, (b) 420 nm and (c) 810 nm.

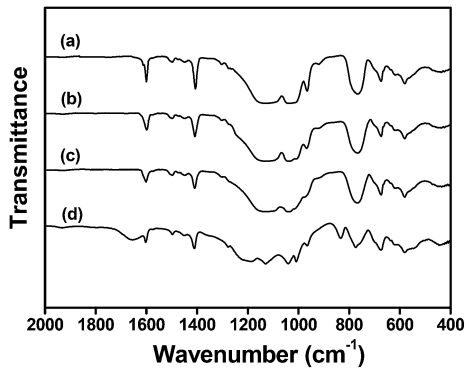

Fig. 3 FT-IR spectra of SiO_2 core particles with an average diameter of (a) 250 nm, (b) 420 nm, (c) 810 nm and (d) core–shell structured SiO_2 particles (core size: 250 nm) encapsulated by poly(sodium-4-styrenesulfonate).

poly(sodium-4-styrenesulfonte) of these core–shell structured SiO_2 particles were replaced with lithium ions by ion exchange. XPS spectra of the resulting core–shell structured SiO_2 particles revealed a 57.4 eV peak characteristic of lithium,[33] indicating that the $SiO_2(Na^+)$ particles were converted to $SiO_2(Li^+)$ particles in the third step, as demonstrated in Fig. 1.

Composite polymer membranes were prepared from P(VdF-*co*-HFP) and core–shell $SiO_2(Li^+)$ particles. A SEM image of the composite polymer membrane containing 20 wt% core–shell $SiO_2(Li^+)$ with a core diameter of 250 nm is shown in Fig. 5(a). The membrane had a homogeneous morphology, and no $SiO_2(Li^+)$ particle agglomeration was observed. The EDS mapping images shown in Fig. 5(b)–(d) also illustrate the homogeneous distributions of specific elements (fluorine, silicone, sulfur) across the image, which suggests that SiO_2 particles were homogeneously distributed in the composite polymer membrane without agglomeration. As the core–shell SiO_2 particles were added into the P(VdF-*co*-HFP) matrix polymer, the mechanical stability was enhanced, which enabled to prepare a free-standing film with sufficient mechanical integrity, as shown in Fig. 6(a). The mechanical properties of the composite polymer membranes were evaluated, and the results are shown in Fig. 6(b). The incorporation of core–shell structured SiO_2 particles into P(VdF-*co*-HFP) membrane improved the tensile strength, however, the enhancement of mechanical strength was not too remarkable, since the composite polymer membranes were very thin (~30 μm). The enhancement of mechanical properties can be ascribed to homogeneous distribution of core–shell SiO_2 particles with high mechanical strength. Permanent covalent bonding between the SiO_2 core and poly(lithium-4-styrenesulfonte) shell resulted in reinforcement of interfacial contacts between the core–shell SiO_2 particles and the P(VdF-*co*-HFP) matrix. The tensile strength was found to be slightly increased with decreasing the core size of SiO_2 particles, which can be ascribed to higher volumetric distribution of core–shell SiO_2 particles with smaller particle size. The volumetric ratio of core–shell SiO_2 particles were 24.8, 22.6 and 19.6% in the composite polymer membranes with $SiO_2(Li^+)$ particles with core diameters of 250, 420 and 810 nm, respectively.

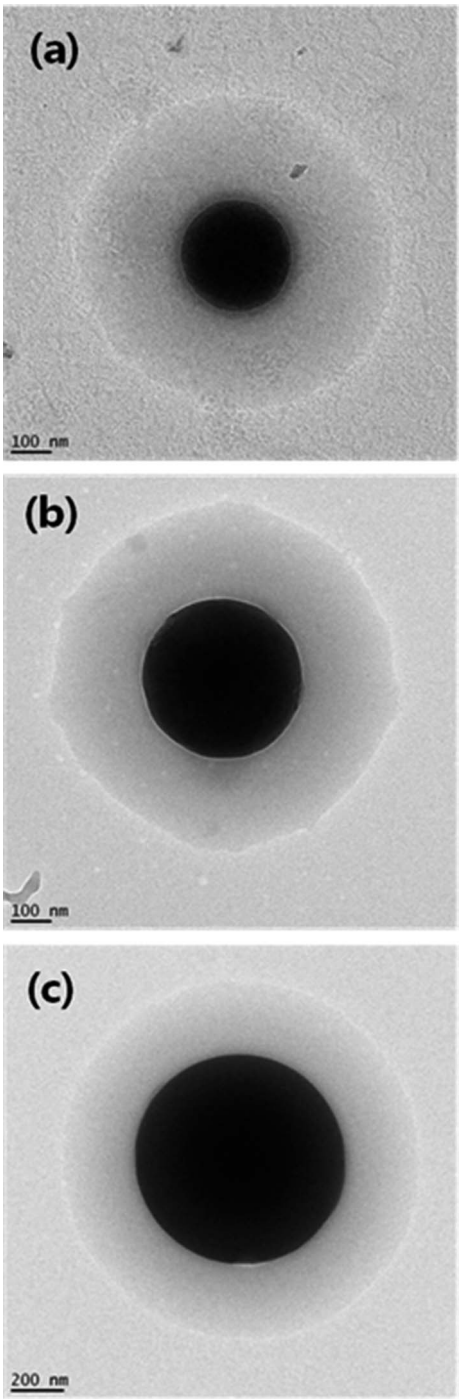

Fig. 4 TEM images of core–shell structured SiO_2 particles with core diameters of (a) 250 nm, (b) 420 nm and (c) 810 nm.

The wettability of the polymer membrane plays an important role in battery performance, because good wettability allows the cell to better retain electrolyte solution, thereby facilitating fast ion transport between the two electrodes during charge and discharge cycling. Photographs were taken of a PP separator and a composite polymer membrane containing 20 wt% $SiO_2(Li^+)$ particles with a core diameter of 250 nm after dropping liquid electrolyte onto their surfaces (Fig. 7). The pristine PP separator was not completely wetted and a liquid droplet was

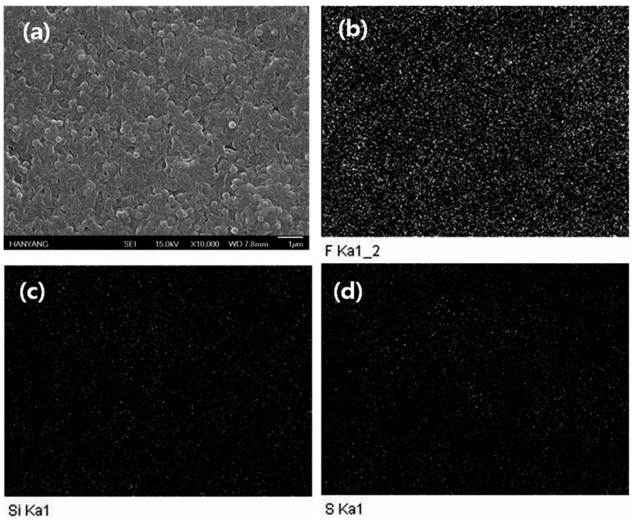

Fig. 5 (a) SEM image and EDAX mapping images of (b) fluorine, (c) silicon and (d) sulfur in the composite polymer membrane containing 20 wt% core–shell structured $SiO_2(Li^+)$ particles with a core diameter of 250 nm.

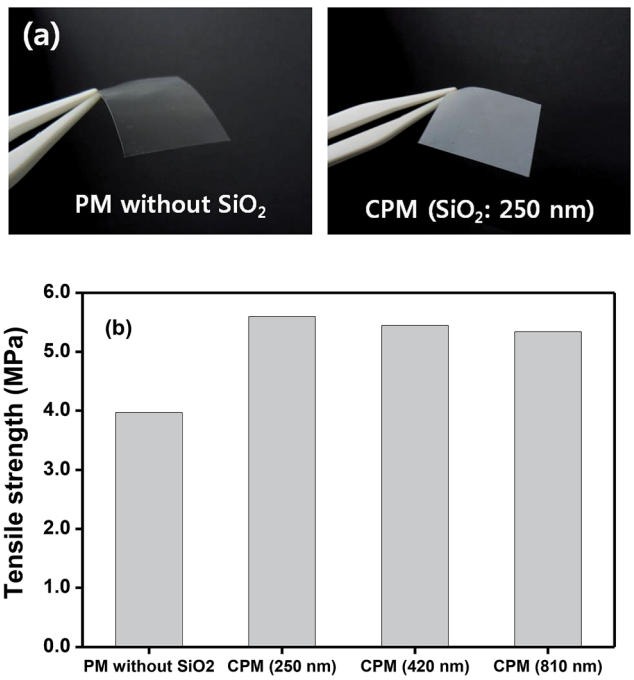

Fig. 6 (a) Photos of polymer membrane without and with core–shell structured SiO_2 particles with a core diameter of 250 nm, and (b) tensile strength of polymer membranes without and with core–shell SiO_2 particles.

observed on its surface, whereas the composite polymer membrane was immediately wetted by the liquid electrolyte. Unlike the PP separator, the electrolyte solution was well encapsulated in the composite polymer electrolyte due to the good compatibility between poly(lithium-4-styrenesulfonte) or P(VdF-*co*-HFP) and liquid electrolyte, which allowed suppression of solvent exudation from the composite polymer electrolyte. For more quantitative comparison, the uptake of electrolyte solution and the ionic conductivities of different composite membranes after soaking in the liquid electrolyte were measured and are summarized in Table 1. The ionic conductivity of the liquid electrolyte used to soak the membranes was 7.0×10^{-3} S cm^{-1}. Note that the ionic conductivity of the PP separator filled with the electrolyte solution (4.6×10^{-4} S cm^{-1}) was much lower than that of the electrolyte solution. It is well known that the ionic conductivity of the separator saturated with liquid electrolyte is decreased due to the combined effects of the separator's tortuosity and porosity. MacMullin number (N_M), the ratio the ionic conductivity of pure liquid electrolyte (σ_0) to that of the separator filled with liquid electrolyte (σ_{eff}), is used to characterize this behavior by the following equation: $N_M = (\sigma_0/\sigma_{eff}) = (\tau^2/\varepsilon)$, where τ is the tortuosity and ε is the porosity of the separator.[34,35] According to previous report,[35] the MacMullin number of separator used in this study (Celgard 2400) is about 16 ± 2, which means that the use of separator sharply decreases the ionic conductivity of liquid electrolyte. In the composite polymer membranes, both electrolyte uptake and ionic conductivity decreased with increasing core diameter of $SiO_2(Li^+)$ particles. Poly(lithium-4-styrenesulfonte), which had a high affinity for the electrolyte solution, was more abundant in $SiO_2(Li^+)$ particles with a smaller core size, resulting in an increase in electrolyte uptake with decreasing core diameter. It can be seen from the data in Table 1 that the lithium transference number increased with an addition of core–shell $SiO_2(Li^+)$ particles. Core–shell $SiO_2(Li^+)$ particle is an intrinsically single ion conductor that transports only Li^+ ions, since the sulfonate anions ($-SO_3^-$) are anchored to pendant groups on the polymer around the silica core. Accordingly, the increase in lithium transference number with an addition of $SiO_2(Li^+)$ particles indicates that the lithium ions dissociated from the $SiO_2(Li^+)$ particles contribute to the ionic conductivity. It is also found that the lithium transference number decreases with increasing core diameter. As the core diameter decreases, the number of lithium ions contributing to ionic conductivity increases, which results in an increase in ionic conductivity and lithium transference number.

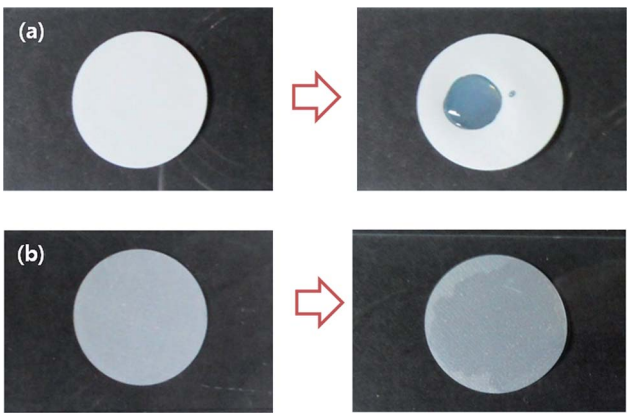

Fig. 7 Photographs of (a) the PP separator and (b) composite polymer membrane (SiO_2 core diameter: 250 nm) after dropping liquid electrolyte onto their surfaces.

Table 1 Electrolyte uptake, ionic conductivities and lithium transference number of the composite polymer electrolytes containing core–shell $SiO_2(Li^+)$ particles with different core diameters

Membrane	Thickness (μm)	Electrolyte uptake (%)	Ionic conductivity (S cm^{-1})	t_{Li+}
PP separator	25	107.5	4.6×10^{-4}	0.31
PM without SiO_2[a]	30	134.6	8.7×10^{-4}	0.35
CPM[b] (SiO_2: 250 nm)	30	193.4	2.3×10^{-3}	0.49
CPM (SiO_2: 420 nm)	30	182.2	1.5×10^{-3}	0.47
CPM (SiO_2: 810 nm)	30	171.3	1.1×10^{-3}	0.44

[a] PM: polymer membrane. [b] CPM: composite polymer membrane. Number in parentheses is the average diameter of the SiO_2 core.

Composite polymer electrolytes containing $SiO_2(Li^+)$ particles were used to assemble lithium-ion polymer cells composed of a graphite negative electrode and a $LiFePO_4$ positive electrode. The cells were initially subjected to a preconditioning cycle in the voltage range of 2.0–3.7 V at the constant current rate of 0.1C. After completing two cycles at the 0.1C rate, the cells were charged at a current density of 0.5C up to a cut-off voltage of 3.7 V. This was followed by a constant-voltage charge with declining current until a final current equal to 10% of the charging current was obtained. The cells were then discharged to a cut-off voltage of 2.0 V at the same current rate. Fig. 8(a) shows the typical charge–discharge curves of the 1st, 20th, 50th, 100th and 200th cycle of the lithium-ion polymer cell assembled with composite polymer electrolyte containing $SiO_2(Li^+)$ particles with a core diameter of 250 nm. The cell delivered an initial discharge capacity of 141.2 mA h g^{-1} based on the active $LiFePO_4$ material in the positive electrode. The cell exhibited stable cycling characteristics; that is, it delivered 92.4% of the initial discharge capacity after 200 cycles. Fig. 8(b) shows the discharge capacity *versus* cycle number of lithium-ion polymer cells assembled with different composite polymer electrolytes. For the purpose of comparison, the cycling results of the cell assembled with liquid electrolyte using a PP separator are also shown. Cells assembled with composite polymer electrolytes exhibited slightly higher initial discharge capacities and better capacity retention than the cell with the liquid electrolyte. As explained earlier, the ionic conductivities of the composite polymer electrolytes were higher than that of a PP separator filled with liquid electrolyte, which was responsible for the increase in initial discharge capacity in the former. In a cell with liquid electrolyte, leakage of the liquid electrolyte may lead to a reduction in ionic conductivity and degradation of the electrolyte/electrode contacts during cycling. In contrast, the composite polymer electrolyte composed of P(VdF-*co*-HFP) and core–shell $SiO_2(Li^+)$ particles contained the organic solvent effectively, which helped to prevent exudation of the electrolyte solution during cycling. In particular, the presence of a large amount of hydrophilic poly(lithium-4-styrenesulfonte) in the shell of the $SiO_2(Li^+)$ particles with a small core size (250 nm) enabled the cell with these particles to retain the solvent more effectively, resulting in good cycling stability. Accordingly, the cell assembled with composite polymer electrolyte containing $SiO_2(Li^+)$ particles with a core diameter of 250 nm exhibited the best cycling performance in terms of initial discharge capacity and capacity retention.

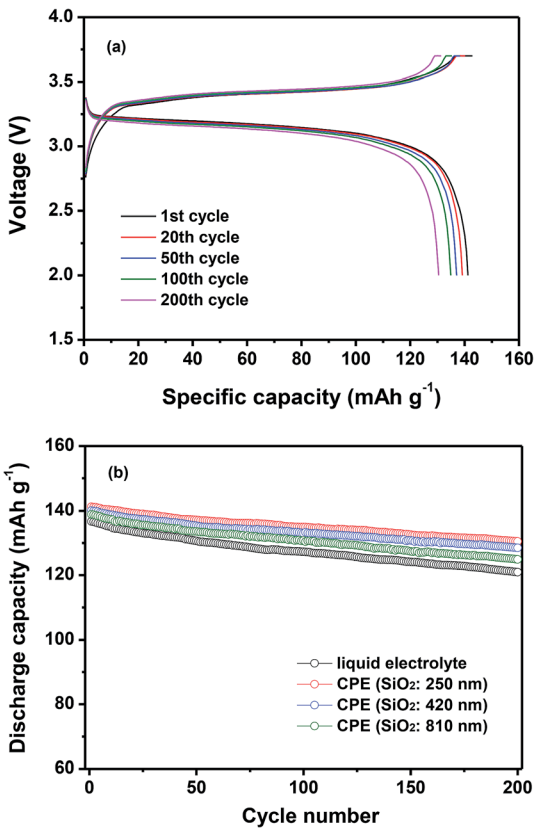

Fig. 8 (a) Charge and discharge curves of a lithium-ion polymer cell assembled with composite polymer electrolyte containing $SiO_2(Li^+)$ particles with a core diameter of 250 nm (0.5C CC and CV charge, 0.5C CC discharge, cut-off: 2.0–3.7 V), and (b) discharge capacities of lithium-ion polymer cells assembled with different electrolytes. CPE refers to composite polymer electrolyte.

Discharge capacities of the lithium-ion polymer cells assembled with different composite polymer electrolytes during experiments in which the C rate was increased every five cycles within the range of 0.1 to 2.0C are compared in Fig. 9. Discharge capacities decreased as the C rate increased, thereby demonstrating polarization. Discharge capacities of the lithium-ion polymer cells with composite polymer electrolytes containing $SiO_2(Li^+)$ particles were higher than those of the liquid electrolyte-based cell for all C rates tested. This superior rate capability can be ascribed to the higher ionic conductivity and better interfacial contacts between electrolyte and electrodes in the lithium-ion polymer cells with composite polymer

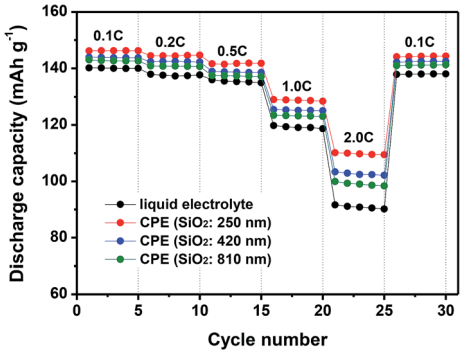

Fig. 9 Discharge capacities of lithium-ion polymer cells assembled with different electrolytes as a function of C rate. The C rate was increased from 0.1 to 2.0C after every 5 cycles.

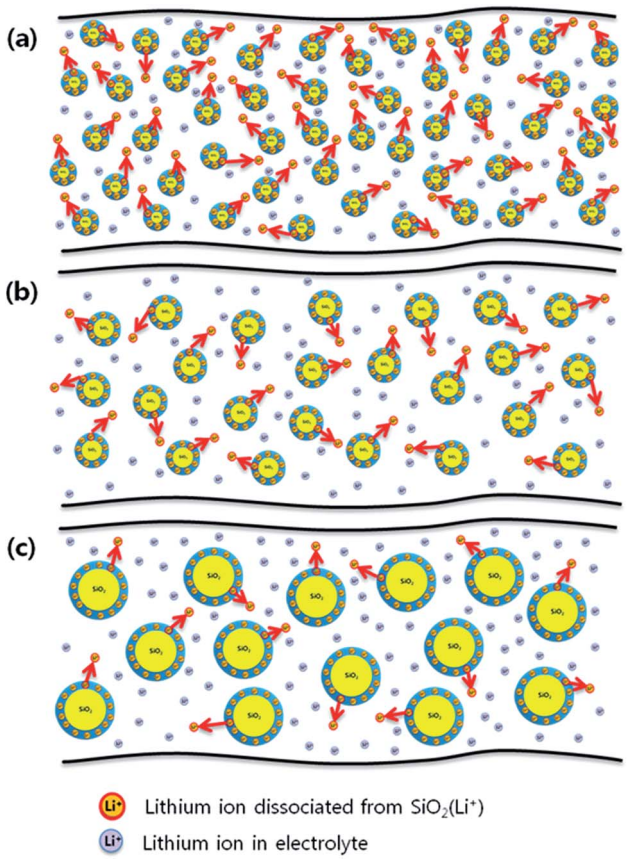

Fig. 10 Schematic presentation of Li^+ ion transport in composite polymer electrolytes containing core–shell structured $SiO_2(Li^+)$ particles with core diameters of (a) 250 nm, (b) 420 nm and (c) 810 nm.

electrolytes than the liquid electrolyte-based cell. Note that the composite polymer electrolyte with $SiO_2(Li^+)$ particles with a core diameter of 250 nm provided the highest capacities at high current rates. As shown in Table 1, the ionic resistance was the lowest and the lithium transference number was the highest in the composite polymer electrolyte containing $SiO_2(Li^+)$ particles with a core diameter of 250 nm, thereby reducing the concentration polarization of the electrolyte during cycling. The cores in the core–shell $SiO_2(Li^+)$ particle are insulators, thus Li^+ ion transport may be blocked by large SiO_2 cores. For this reason, the connectivity of the ion-conducting phase becomes more tortuous in composite polymer electrolyte containing $SiO_2(Li^+)$ particles with a large core size (Fig. 10). Thus, the best rate performance was delivered by the cell assembled with $SiO_2(Li^+)$ particles with a 250 nm core diameter. The cell recovered 98.7% of the initial discharge capacity at the rate of 0.1C after high current rate cycles, indicating that it had good cycling stability. These results indicate that composite polymer electrolyte containing core–shell SiO_2 particles with an optimized core diameter is a promising electrolyte material for high performance lithium-ion polymer batteries with good cycling stability.

Conclusions

Core–shell structured SiO_2 particles with different core diameters were synthesized and used as Li^+-conducting fillers in composite polymer electrolytes. Composite polymer electrolytes prepared with P(VdF-*co*-HFP) and core–shell $SiO_2(Li^+)$ particles exhibited high ionic conductivity and good mechanical strength for use in rechargeable lithium-ion polymer cells. Lithium-ion polymer cells assembled with a graphite negative electrode, a composite polymer electrolyte containing $SiO_2(Li^+)$ particles with an optimized core size, and a $LiFePO_4$ positive electrode were characterized by high discharge capacity, good cycling stability and good high rate performance.

Acknowledgements

This work was supported by Basic Science Research Program through the National Research Foundation of Korea (NRF) funded by the Ministry of Science, ICT and future Planning (2014R1A2A2A01002154) and by a grant of the Human Resources Development Program of KETEP, funded by the Ministry of Trade, Industry and Energy of Korea (no. 20124010203290).

References

1 M. B. Armand, *Solid State Ionics*, 1994, **69**, 309.
2 J. Hassoun, P. Reale and B. Scrosati, *J. Mater. Chem.*, 2007, **17**, 3668.
3 J. W. Fergus, *J. Power Sources*, 2010, **195**, 4554.
4 E. Quartarone and P. Mustarelli, *Chem. Soc. Rev.*, 2011, **40**, 2525.
5 H. Zhang, X. Ma, C. Lin and B. Zhu, *RSC Adv.*, 2014, **4**, 33713.
6 *Polymer Electrolyte Review*, ed. J. R. MacCallum and C. A. Vincent, Elsevier Applied Science, London, 1987 and 1989, vol. 1 and 2.
7 F. M. Gray, *Polymer Electrolytes*, The Royal Society of Chemistry, Cambridge, 1997.
8 J.-M. Tarascon and M. Armand, *Nature*, 2001, **414**, 359.
9 J. Y. Song, Y. Y. Wang and C. C. Wan, *J. Power Sources*, 1999, **77**, 183.
10 A. M. Stephan, *Eur. Polym. J.*, 2006, **42**, 21.
11 J. Fan and P. S. Fedkiw, *J. Electrochem. Soc.*, 1997, **144**, 399.
12 D. W. Kim and Y. K. Sun, *J. Electrochem. Soc.*, 1998, **145**, 1958.

13 F. Croce, G. B. Appetecchi, L. Persi and B. Scrosati, *Nature*, 1998, **394**, 456.
14 N. Byrne, J. Efthimiadis, D. R. MacFarlane and M. Forsyth, *J. Mater. Chem.*, 2004, **14**, 127.
15 A. S. Arico, P. Bruce, B. Scrosati, J.-M. Tarascon and W. Van Schalkwijk, *Nat. Mater.*, 2005, **4**, 366.
16 S. K. Das, S. S. Mandal and A. J. Bhattacharyya, *Energy Environ. Sci.*, 2011, **4**, 1391.
17 Z. Jia, W. Yuan, H. Zhao, H. Hu and G. L. Baker, *RSC Adv.*, 2014, **4**, 41087.
18 N. S. Choi, Y. M. Lee, B. H. Lee, J. A. Lee and J. K. Park, *Solid State Ionics*, 2004, **167**, 293.
19 J. Nordstrom, A. Matic, J. Sun, M. Forsyth and D. R. MacFarlane, *Soft Matter*, 2010, **6**, 2293.
20 Y. S. Lee, S. H. Ju, J. H. Kim, S. S. Hwang, J. M. Choi, Y. K. Sun, H. Kim, B. Scrosati and D. W. Kim, *Electrochem. Commun.*, 2012, **17**, 18.
21 Y. S. Lee, J. H. Lee, J. A. Choi, W. Y. Yoon and D. W. Kim, *Adv. Funct. Mater.*, 2013, **23**, 1019.
22 S. H. Ju, Y. S. Lee, Y. K. Sun and D. W. Kim, *J. Mater. Chem. A*, 2013, **1**, 395.
23 K. Padhi, K. S. Nanjundaswamy and J. B. Goodenough, *J. Electrochem. Soc.*, 1997, **144**, 1188.
24 H. Joachin, T. D. Kaun, K. Zaghib and J. Prakash, *J. Electrochem. Soc.*, 2009, **156**, A401.
25 L.-X. Yuan, Z.-H. Wang, W.-X. Zhang, X.-L. Hu, J.-T. Chen, Y.-H. Huang and J. B. Goodenough, *Energy Environ. Sci.*, 2011, **4**, 269.
26 Y. Park, K. C. Roh, W. Shin and J. W. Lee, *RSC Adv.*, 2013, **3**, 14263.
27 J. Evance, C. A. Vincent and P. G. Bruce, *Polymer*, 1987, **28**, 2324.
28 J. P. Blitz, R. S. S. Murthy and D. E. Leyden, *J. Colloid Interface Sci.*, 1988, **121**, 63.
29 P. Siberzan, L. Leger, D. Ausserre and J. J. Benatta, *Langmuir*, 1991, **7**, 1647.
30 C. P. Tripp and M. L. Hair, *Langmuir*, 1992, **8**, 1120.
31 J. C. Yang, M. J. Jablonsky and J. W. Mays, *Polymer*, 2002, **43**, 5125.
32 E. B. Orler, D. J. Yontz and R. B. Moore, *Macromolecules*, 1993, **5157**, 26.
33 S. H. Goh, S. Y. Lee, X. Luo and C. H. A. Huan, *Polymer*, 2000, **41**, 211.
34 P. Arora and Z. Zhang, *Chem. Rev.*, 2004, **104**, 4419.
35 D. Djian, F. Alloin, S. Martinet, H. Lignier and J. Y. Sanchez, *J. Power Sources*, 2007, **172**, 416.

